Characterization of electrodeposited $Zn_{1-x}Hg_xSe$ thin films

2005 Semicond. Sci. Technol. 20 749

(http://iopscience.iop.org/0268-1242/20/8/017)

INSTITUTE OF PHYSICS PUBLISHING SEMICONDUCTOR SCIENCE AND TECHNOLOGY

Semicond. Sci. Technol. **20** (2005) 749–754 doi:10.1088/0268-1242/20/8/017

Characterization of electrodeposited $Zn_{1-x}Hg_xSe$ thin films

T Mahalingam[1,4], A Kathalingam[1], S Velumani[2], Soonil Lee[3], Kyeung Seek Lew[4] and Yong Deak Kim[4]

[1] Department of Physics, Alagappa University, Karaikudi-630 003, India
[2] Mexican Institute of Petroleum, Eje Central 152, CP 07730, México, DF, Mexico
[3] Department of Molecular Science and Technology, Ajou University, Suwon 442-749, Korea
[4] Department of Electrical and Computer Engineering, College of Information Technology, Ajou University, Suwon 443-749, Korea

Received 29 March 2005, in final form 29 April 2005
Published 6 June 2005
Online at stacks.iop.org/SST/20/749

Abstract

In this work the synthesis of zinc mercury selenide thin films ($Zn_{1-x}Hg_xSe$) by electrodeposition is carried out. The films were deposited onto conducting glass (SnO_2) substrates from an aqueous solution bath containing $ZnSO_4$, $HgCl_2$ and SeO_2 at bath temperatures between 30 °C and 70 °C. The influence of deposition parameters such as electrolyte composition, deposition potential and temperature on the crystallinity and composition of the films is studied. It is found that the amount of mercury content in the solution bath and deposition potential control the composition and structure of the alloy films. The films were characterized by x-ray diffraction (XRD), energy dispersive x-ray analysis (EDAX), optical absorption and scanning electron microscope (SEM) studies. Photoelectrochemical solar cells studies using $Zn_{1-x}Hg_xSe$ thin films showed improved performance for annealed and etched electrodes and the results are discussed.

1. Introduction

Alloys of II–VI compounds are potential candidates for opto-electronic device applications [1]. Recently, ternary compounds have received much attention in the field of solar cells owing to their interesting properties of band gap and lattice constant modulation by composition. Among the II–VI ternary compounds, ZnCdSe and CdHgTe (with higher Hg content) have been studied widely for solar cells and IR device application [2, 3]. Even though CdHgTe has been well studied in the past, little work has been reported on thin films of zinc mercury selenide (ZnHgSe). Epitaxial layers of $Zn_{1-x}Hg_xSe$ on GaAs substrates by gas-source MBE were grown and studied for application as an active layer in blue-green QW lasers [4]. Dharmadasa *et al* [5] studied the growth of n- and p-type ZnSe thin films for light emitting devices and multi-layer tandem solar cells. Samantilleke *et al* [6] reported the development of opto-electronic devices using electrochemically grown thin ZnSe layers. $Zn_{1-x}Hg_xSe$ thin film systems formed with excess electrical carriers could be used for the fabrication of opto-electronic devices such as solar cells. In the case of photon energy converters, it is possible to tailor the match between the solar spectrum and the characteristics of the absorber. Due to their wide range of band gaps, ZnSe and HgSe could form as a solid solution alloy of $Zn_{1-x}Hg_xSe$ with the possibility of tailoring the band gap in a wide range for using them in solar cell applications. Though it has potential advantages over other alloys, the work reported on thin films of this system is limited. This motivated us to synthesize and study the material properties in thin film form. Even though several sophisticated thin film deposition techniques are available, the electrodeposition technique now emerges as an important low cost and low temperature method to synthesize semiconducting compound and alloy thin films [7]. The electrodeposition of II–VI ternary compounds is more complex as they involve several deposition parameters, which control the film properties such as film composition and structure. Hence, we have carried out a systematic study in this work to analyse the deposition conditions to grow $Zn_{1-x}Hg_xSe$ alloy films. The influence of deposition conditions such as elelctrolyte concentration, especially $HgCl_2$ in the bath solution, deposition potential and bath temperature on the film composition, structure and morphology is studied.

2. Experimental details

All chemicals used in this work were of analytical reagent grade (99% purity, E-Merck). Zinc mercuric selenide ($Zn_{1-x}Hg_xSe$) thin films were deposited onto fluorine doped tin oxide coated glass substrates (15 Ω/square) from an aqueous solution bath containing 20 to 50 mM of $ZnSO_4$, 1 to 4 mM of SeO_2 and 0.2 to 1 mM of $HgCl_2$ in the pH range between 2 and 4. The substrates were cleaned with acetone and methanol, and rinsed in distilled water prior to deposition. Depositions were carried out cathodically using a scanning potentiostat (Model 362, EG&G, Princeton Applied Research, USA). A standard three-electrode system comprising a graphite rod and saturated calomel electrode (SCE) was used for the depositions as counter and reference electrodes, respectively. During deposition the bath solution was stirred slowly using a magnetic stirrer with hot plate. 100 ml of electrolyte solution was taken in a beaker; the reference electrode was introduced into the solution with Luggin capillary arrangement. After film formation, the samples were rinsed with distilled water, dried and stored in a desiccator for further studies. The film thickness was measured using multiple beam interferometry and microbalance techniques. The deposited films were analysed using x-ray diffraction (XRD) by Bruker Discover D8 diffractometer using CuK_α radiation with $\lambda = 0.154\,18$ nm. Surface morphological and compositional analyses were carried out using a scanning electron microscope and energy dispersive x-ray analysis set-up (EDAX) attached with SEM, respectively (Philips, Model XL 30). Optical measurements were carried out using a JASCO V-570 spectrophotometer. ZnHgSe thin films were annealed in air at 300 °C for 15 min. The conductivity type was measured using a hot probe technique and all the alloy films of $Zn_{1-x}Hg_xSe$ exhibited n-type behaviour. The annealed ZnHgSe photoelectrode was etched chemically by immersing the electrode in 2.5 M HCl for 10 s and rinsed in deionized water. A photoelectrochemical (PEC) solar cell was fabricated using $Zn_{1-x}Hg_xSe$ films as the working electrode in a three-electrode arrangement consisting of a carbon rod and SCE as counter and reference electrodes, respectively, in 0.25 M polyiodide (NaOH-KI-I_2) electrolyte. The solar cell power characteristics were found using a 150 W tungsten–halogen lamp.

3. Results and discussion

$Zn_{1-x}Hg_xSe$ films with thickness in the range between 0.3 and 1.2 μm were grown at bath temperature 70 °C. The deposited films are found to be shiny grey in colour and adhered well to the substrates. The optimum deposition conditions to synthesize $Zn_{1-x}Hg_xSe$ thin films are identified as: deposition potential −0.7 V versus SCE, solution pH: 3.0 ± 0.1, bath temperature 70 °C, electrolyte concentration 30 mM $ZnSO_4$, 2 mM SeO_2 and 0.8 mM $HgCl_2$.

3.1. Cyclic voltammetric studies

Cyclic voltammetry is a powerful tool for the study of electrochemical depositions. Figures 1(*a*), (*b*) and (*c*) show the voltammograms recorded for Se, HgSe and ZnHgSe systems on tin oxide coated glass substrates, respectively. In curve

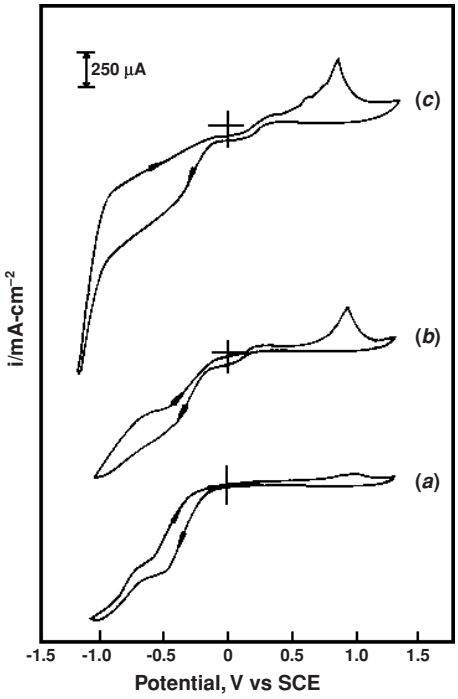

Figure 1. Cyclic voltammograms on tin oxide coated electrodes in (*a*) 3 mM SeO_2, (*b*) 3 mM SeO_2 + 1 mM $HgCl_2$ and (*c*) 3 mM SeO_2 + 1 mM $HgCl_2$ + 50 mM $ZnSO_4$.

(*a*), the wave centred around −0.5 V may be attributed to the reduction of selenous acid. In curve (*b*), the wave centred on 0 V corresponds to the reduction of Hg^{2+} to Hg and another wave around −0.4 V is likely due to the formation of HgSe. The anodic peak in this curve corresponds to the stripping of deposited HgSe in the reverse scan. The reduction of all the three precursors is shown in figure 1(*c*). The wave around −0.4 V corresponds to the formation of HgZnSe layers and the cathodic current increases gradually up to −1.0 V indicating the growth of HgZnSe layers. Beyond −1.0 V, the current increases rapidly indicating the hydrogen evolution, and it has been found that the deposits obtained at potentials below −1.0 V are not adhered to the substrates and found to be peeled out due to hydrogen evolution. The anodic peak around +0.8 V corresponds to the stripping of deposited HgZnSe layers in the reverse scan. Based on the above results, the deposition potential in the range between −0.4 and −1.0 V versus SCE has been selected to synthesize HgZnSe thin films in the present work.

3.2. Effect of bath temperature and pH

The bath temperature plays a vital role in the electrodeposition and properties of semiconducting alloy thin films. The bath temperature is expected to influence the deposition rate by increasing the diffusion coefficient of the species and precursor solubility [8]. $Zn_{1-x}Hg_xSe$ thin films deposited at low bath temperatures (<50 °C) are found to be poorly crystallized and amorphous in nature. $Zn_{1-x}Hg_xSe$ alloy thin films deposited at a bath temperature 70 °C are found to exhibit well-defined peaks corresponding to the alloy in the x-ray diffractograms. The current densities were found to increase at higher bath temperatures yielding thicker deposits. The deposition rate

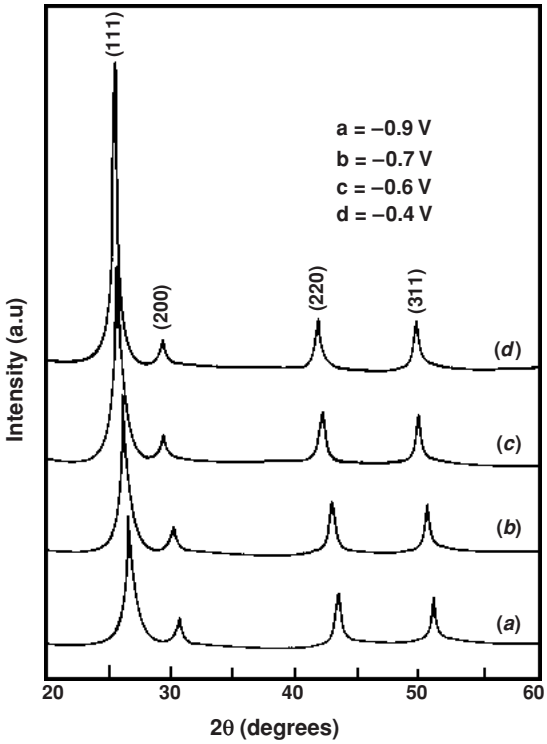

Figure 2. X-ray diffraction patterns of $Zn_{1-x}Hg_xSe$ films deposited at various potentials (bath composition: 2 mM SeO_2, 0.8 mM $HgCl_2$, 30 mM $ZnSO_4$; bath temperature: 70 °C; pH: 3.0 ± 0.1).

of typical HgZnSe thin films is estimated to be 17 nm min^{-1} at a bath temperature of 70 °C. pH values between 2 and 4 were employed to deposit the $Zn_{1-x}Hg_xSe$ thin films. At pH below 1.5, hydrogen evolution hindered the film growth and adherence of deposited films to the substrates was poor. Also, at pH > 4, film growth rate reduces due to smaller current densities. Films deposited at pH 3 have yielded significant results when used in PEC solar cells. Hence, the bath temperature and solution pH were fixed as 70 °C and 3, respectively, for further deposition and characterization of $Zn_{1-x}Hg_xSe$ thin films in the present work.

3.3. Effect of deposition potential

$Zn_{1-x}Hg_xSe$ films were deposited at different potentials ranging from −0.4 V to −1.0 V versus SCE. The deposition potential is found to influence the structural behaviour of $Zn_{1-x}Hg_xSe$ thin films. Figure 2 shows the XRD patterns of the films deposited at various deposition potentials in the range between −0.4 and −1.0 V versus SCE. X-ray diffraction spectra of $Zn_{1-x}Hg_xSe$ films are found to be polycrystalline with a cubic structure. It is found that the cubic (111) peak increases with the deposition potential in the range −1.0 to −0.4 V versus SCE and also shifts slightly towards lower diffraction angles. This increase of the (111) peak at more positive potentials is attributed to the Hg-rich films; HgSe gives a larger diffraction signal due to its crystalline quality and higher absorption coefficient for x-rays. The shifting of the x-ray diffraction peaks towards low diffraction angles with the increase of deposition potential may be attributed to the increase of mercury content in the films. When the films

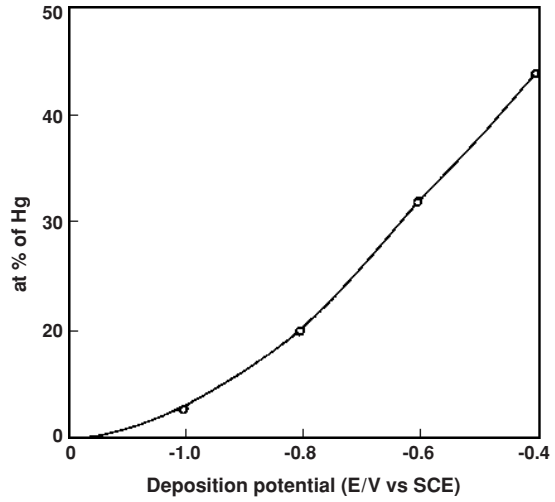

Figure 3. Mercury content in the films (at%) as a function of deposition potential (bath composition: 2 mM SeO_2, 0.8 mM $HgCl_2$, 30 mM $ZnSO_4$; bath temperature: 70 °C; pH: 3.0 ± 0.1).

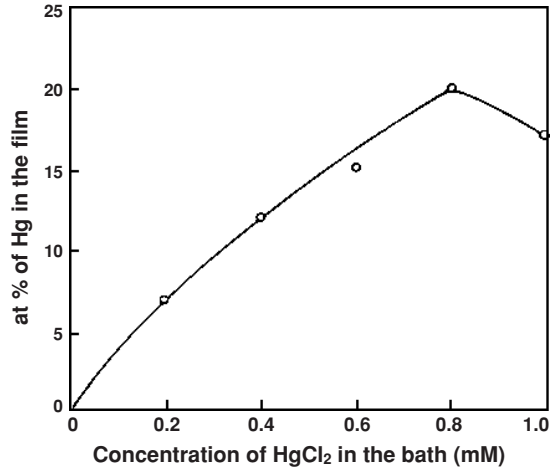

Figure 4. Mercury content in the films (at%) as a function of $HgCl_2$ in the solution bath (deposition potential: −0.7 V versus SCE, bath temperature: 70 °C; pH: 3.0 ± 0.1, bath composition: 2 mM SeO_2, 30 mM $ZnSO_4$).

are deposited at more negative potentials (<−1.0 V versus SCE), hydrogen evolution hinders the plating efficiency with a possible reduction of Se to Se^{2-} that in turn reduces the (111) peak height and crystallinity of deposited $Zn_{1-x}Hg_xSe$ films. Visible deposition of Zn occurred at potentials less than −1.0 V, whereas for potentials greater than −0.6 V the films showed an excess of Se. The atomic percentage of Hg in the films deposited at various potentials is shown in figure 3. It is observed that Hg-rich and Zn-rich films are deposited at more positive (⩾−0.6 V) and more negative (⩽−0.8 V) potentials, respectively. The mercury content in the films is found to increase with the deposition potential which may be attributed to the noble nature and more positive deposition potential of mercury compared to selenium and zinc.

3.4. Influence of bath concentration

Figure 4 shows the variation of mercury content in the film with $HgCl_2$ concentration in the deposition bath for films

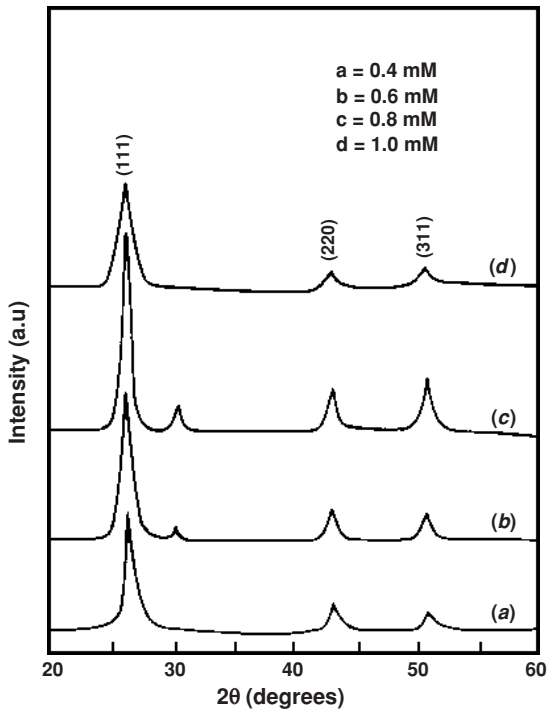

Figure 5. X-ray diffraction patterns of films deposited with various $HgCl_2$ concentrations in the solution bath (deposition potential: −0.7 V versus SCE, bath temperature: 70 °C; pH: 3.0 ± 0.1, bath composition: 2 mM SeO_2, 30 mM $ZnSO_4$).

deposited at a potential −0.7 V versus SCE. The content of mercury in the film depends on the concentration of $HgCl_2$ in the bath at a particular deposition potential. Increasing the bath concentration of mercury has shown well-pronounced diffraction peaks of $Zn_{1-x}Hg_xSe$ thin films. When the $HgCl_2$ in the solution bath reaches 1 mM, the mercury content in the film becomes practically constant. For a fixed bath composition of mercury, higher mercury content is obtained at more positive potentials.

The XRD patterns of films with various mercury concentrations in the deposition bath deposited at −0.7 V versus SCE are represented in figure 5. X-ray diffraction patterns of the films are cubic with (111) orientation for all the films deposited at various $HgCl_2$ concentrations. The intensity of the (111) peak is found to increase with $HgCl_2$ content and exhibited a maximum for the film with a $HgCl_2$ content of 0.8 mM and further increase of $HgCl_2$ to 1.0 mM is found to reduce the intensity of (111) and other peaks. The decrease in the XRD peak heights of the films with high mercury concentrations in the solution bath indicates a lower Faradic efficiency.

The effects of SeO_2 concentration in the bath solution on the x-ray diffraction patterns of $Zn_{1-x}Hg_xSe$ thin films are also studied. It is found that there is no change in the position of diffraction peaks for the variation of SeO_2 concentration in the solution bath. However, the height of the diffraction peaks increases linearly with SeO_2 concentration and it reaches a limiting value after 2 mM (results not shown). It is found that there is no major influence in the XRD patterns of the films due to concentration of $ZnSO_4$ in electrolyte solution except a very small decrease in the height of the diffraction peaks when the

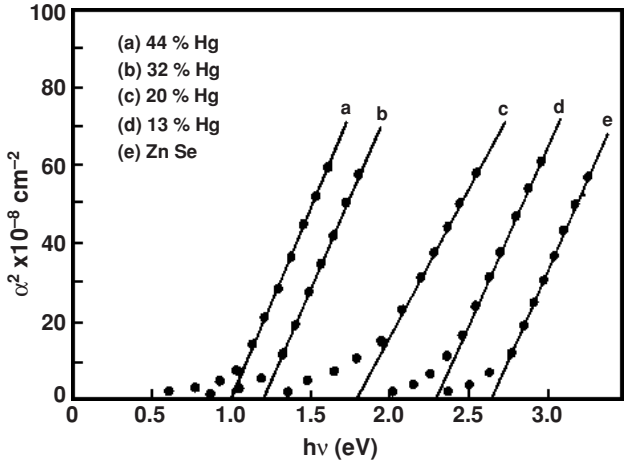

Figure 6. Plots of $(\alpha h\nu)^2$ versus $h\nu$ for various $Zn_{1-x}Hg_xSe$ film compositions.

concentration increases above 40 mM. At higher concentration of $ZnSO_4$ (above 40 mM), increased hydrogen evolution was observed and the deposits were found to be irregular. In the present investigation, the concentrations of SeO_2 and $ZnSO_4$ are kept as 2 mM and 30 mM, respectively, to prepare films for all the other characterizations and fabricating thin film photoelectrochemical solar cells.

3.5. Optical studies

Optical transmittance measurements of the films were used to estimate the band gap energy from the position of the absorption edge and it was found to change with alloy composition x in $Zn_{1-x}Hg_xSe$ thin films. The transmittance spectra obtained for $x = 0.13$, 0.20, 0.32 and 0.44 indicated a shift of absorption edge to longer wavelengths. The optical absorption data were used to plot a graph of $(\alpha h\nu)^2$ versus $h\nu$, where α is the optical absorption coefficient of the material and $h\nu$ is the photon energy. Extrapolation of the plots to the x-axis gives the energy band gap of the deposited films of various compositions as shown in figure 6. The band gap of ZnSe thin films obtained in this work (2.65 eV) is in agreement with the value reported for vacuum evaporated [9] and electrodeposited [10] ZnSe thin films. As the value of mercury content in the film (x) increases, the band gap is shifted to lower values and band gap tailoring is achieved in the alloy films.

3.6. Surface morphological studies

Figure 7(*a*) shows a scanning electron micrograph of typical $Hg_{0.8}Zn_{0.2}Se$ thin film in the as-grown condition. The micrograph exhibits a smooth surface with spherical shaped grains. Several small grains are found to agglomerate and form a few larger grains. The average sizes of smaller grains are found to be in the range between 50 and 100 nm. Figure 7(*b*) shows a scanning electron micrograph of a typical $Hg_{0.8}Zn_{0.2}Se$ film annealed in air at 300 °C for 15 min. The grains are found to be larger due to fusion of small crystallites and recrystallization due to annealing. The average grain sizes are around 1 μm and found to be increased significantly due to annealing process.

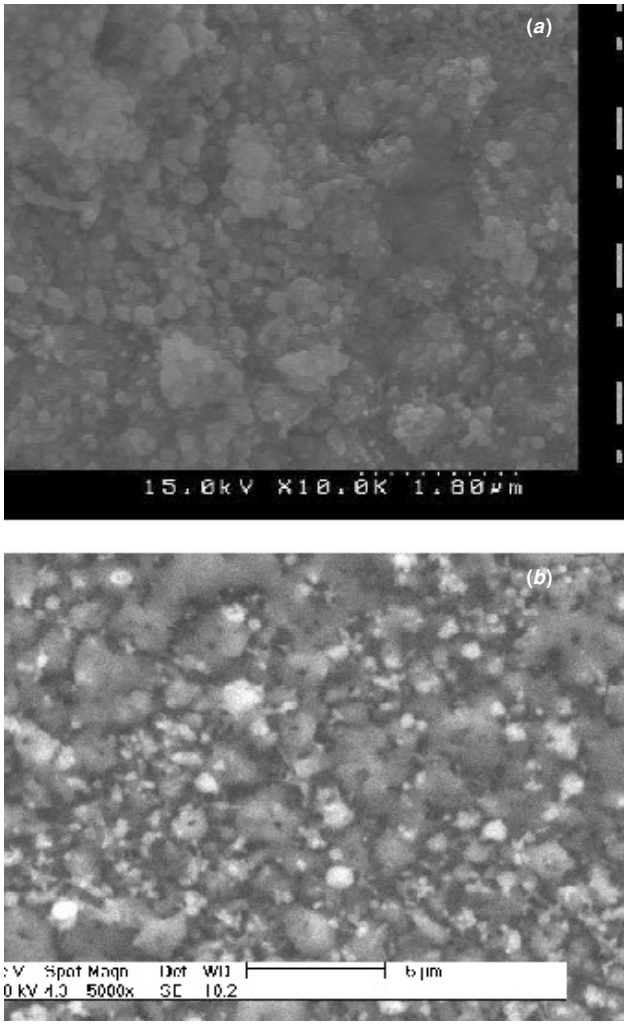

Figure 7. Scanning electron micrographs of typical $Zn_{1-x}Hg_xSe$ thin films: (*a*) as-grown and (*b*) annealed.

3.7. Effect of annealing

The improvement of microstructure of $Hg_{0.8}Zn_{0.2}Se$ films due to annealing is evidenced by the SEM micrograph shown in figure 7(*b*). Annealing the films up to 300 °C increases the diffraction intensities of the prominent peaks and this indicates the enhancement of crystallite size. However, annealing above 300 °C reveals a reduction in mercury content. The increase of the intensity of the XRD signal after annealing treatment can be explained by the crystallization of some amorphous $Zn_{1-x}Hg_xSe$ formed beside the crystalline $Zn_{1-x}Hg_xSe$ during electrodeposition.

3.8. Photoelectrochemical solar cell studies

Photoelectrochemical solar cells comprising typical as-grown, annealed (300 °C in air for 15 min), and annealed and chemically etched $Hg_{0.8}Zn_{0.2}Se$ thin films were constructed and studied. As-deposited $Zn_{1-x}Hg_xSe$ photoelectrode at room temperature in the bath did not reveal measurable electric output and this might be attributed to the small crystallite sizes in the films. However, $Zn_{1-x}Hg_xSe$ thin film deposited at a high bath temperature (70 °C) is found to be crystalline

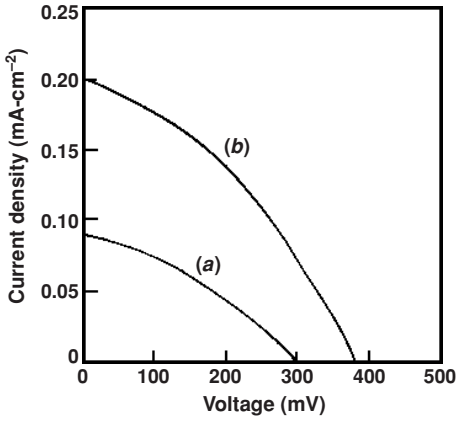

Figure 8. Power characteristics of typical $Hg_{0.8}Zn_{0.2}Se$ PEC solar cells: (*a*) annealed and (*b*) annealed and chemical etched.

Table 1. Solar cell parameters evaluated using the power output plot.

Sl no	Film conditions	V_{oc} (mV)	J_{sc} (mA cm^{-2})	FF	Efficiency (η%)
1	Annealed	300	0.09	0.40	0.50
2	Annealed & etched	383	0.20	0.51	0.65

and photoactive in nature. The power characteristics of PEC solar cells using annealed and etched $Hg_{0.8}Zn_{0.2}Se$ thin film electrodes are shown in figure 8. The efficiency of solar cells is represented by the expression,

$$\eta = V_{oc} J_{sc} \mathrm{FF} 100 / P$$

in which the fill factor (FF) is given by

$$\mathrm{FF} = V_m J_m / V_{oc} J_{sc}$$

where V_{oc} and J_{sc} are the open circuit voltage and short circuit current density, respectively. V_m and J_m are the voltage and current at the maximum power point of the solar cell and P is the input power. The solar cell parameters obtained in the present investigation are shown in table 1. Annealing of the photoelectrode leads to increase in grain size, which reduces the grain boundaries in the film structure. As a result, the diffusion length of the charge carriers increases leading to an improved fill factor and efficiency of the solar cells. When the annealed film is subjected to chemical etching, the fill factor and efficiency are found to improve significantly. During the chemical etching, etch pits are created on the photoelectrode surface, which in turn increases the effective area of photoelectrode surface in contact with the electrolyte for producing the photovoltage in a liquid junction solar cell. Etching also removes dislocations, surface states in the photoelectrode and leads to an increased conversion efficiency of the PEC solar cell [11]. Even though improved performance is obtained for annealed and etched photoelectrodes, the overall solar cell efficiency is still found to be low. Further studies, such as optimization and

surface modification of electrodes, to improve the efficiency of photoelectrochemical solar cells based on $Zn_{1-x}Hg_xSe$ thin films at various compositions are currently in progress.

4. Conclusions

$Zn_{1-x}Hg_xSe$ alloy thin films with x values ranging from 0.13 to 0.44 were successfully electrodeposited onto tin oxide coated conducting glass substrates. A cyclic voltammetry study is used to fix the deposition potential in the range from -0.4 to -1.0 V versus SCE to co-deposit $Zn_{1-x}Hg_xSe$ films. The film composition is found to be modulated by changing the mercury content in the solution bath and deposition potential. X-ray diffraction studies revealed the formation of polycrystalline $Zn_{1-x}Hg_xSe$ alloys with a preferred orientation along the (111) plane. Optical measurements revealed a band gap tailoring when the mercury content in the films is varied in the range between 0.13 and 0.44. Photoelectrochemical solar cells using $Hg_{0.8}Zn_{0.2}Se$ revealed a higher efficiency for the annealed and etched electrode.

References

[1] Cobb S D, Szofran F R, Jones K S and Lehoczky S L 1999 *J. Electron. Mater.* **28** 732
[2] Gaines J M, Drenten R R, Haberern K W, Marshell T, Mensz P and Petruzzello J 1993 *Appl. Phys. Lett.* **62** 2462
[3] Cobb S D, Andrews R N, Szofran F R and Lehoczky S L 1991 *J. Cryst. Growth* **110** 415
[4] Hara K, Machimura H, Usui M, Munekata H and Kukimoto H 1995 *Appl. Phys. Lett.* **66** 3337
[5] Dharmadasa I M, Samantilleke A P, Young J, Boyle M H, Bacewicz R and Wolska A 1995 *J. Mater. Sci. Mater. Electron.* **10** 441
[6] Samantilleke A P, Dharmadasa I M, Prior K A, Choy K L, Mei J, Bacewicz R and Wolska A 2001 *J. Mater. Sci. Mater. Electron.* **12** 661
[7] Gu Z H and Tahdy T Z 1999 *J. Electrochem. Soc.* **146** 156
[8] Koningstein C and Newmann-Spallart M 1998 *J. Electrochem. Soc.* **145** 337
[9] Garcia V M, Nair M T S and Nair P K 1999 *Semicond. Sci. Technol.* **14** 366
[10] Samantilleke A P, Boyle M H, Young J and Dharmadasa I M 1998 *J. Mater. Sci. Mater. Electron.* **9** 231
[11] Gerischer H 1975 *Electrochim. Acta* **58** 263